

Dark soliton past a finite-size obstacle

Nicolas Bilas and Nicolas Pavloff

Laboratoire de Physique Théorique et Modèles Statistiques¹,
Université Paris Sud, bât. 100, F-91405 Orsay Cedex, France

Abstract

We consider the collision of a dark soliton with an obstacle in a quasi-one-dimensional Bose condensate. We show that in many respects the soliton behaves as an effective classical particle of mass twice the mass of a bare particle, evolving in an effective potential which is a convolution of the actual potential describing the obstacle. Radiative effects beyond this approximation are also taken into account. The emitted waves are shown to form two counterpropagating wave packets, both moving at the speed of sound. We determine, at leading order, the total amount of radiation emitted during the collision and compute the acceleration of the soliton due to the collisional process. It is found that the radiative process is quenched when the velocity of the soliton reaches the velocity of sound in the system.

PACS numbers:

03.75.-b Matter waves

05.60.Gg Quantum transport

42.65.Tg Optical solitons; nonlinear guided waves

¹Unité Mixte de Recherche de l'Université Paris XI et du CNRS (UMR 8626).

1 Introduction

One of the many interesting aspects of the physics of Bose-Einstein condensation of ultracold atomic vapors is to open opportunities of studying mesoscopiclike phenomena in new types of setups. The advances in the production and propagation of Bose-Einstein condensates in more and more elaborate waveguides (magnetic or optical, microfabricated or not [1]) opens up the prospect of studying a rich variety of quantum transport phenomena for these intrinsically phase-coherent, finite-sized systems. In particular it has been possible to study quantum interference effects [2], Bloch oscillations and Landau-Zener tunneling [3], Josephson junctions [4], and superfluidity [5].

Pushing further the analogy in transport properties of mesoscopic systems and Bose-condensed vapors, one notices that, whereas in mesoscopic physics interaction effects are often difficult to understand, in Bose-Einstein condensates they are more easily accessible to theoretical description and have the advantage of covering a wide range of regimes, ranging from almost noninteracting atom lasers to strongly correlated systems. Along this line, the existence of nonlinearity in the wave equation, resulting in the existence of bright [6] a dark [7] solitons, appears as a natural – and rather simply understood – consequence of interaction on transport phenomena of quasi-one-dimensional Bose-condensed systems.

In the present work we address the problem of transport of a dark soliton in a quasi-one-dimensional Bose-Einstein condensate. More precisely, we consider a guided Bose-Einstein condensate and theoretically study the propagation of a dark soliton encountering an obstacle on its way. In the appropriate limit [see Eq. (1) below] the system is described by a one-dimensional nonlinear Schrödinger equation. This equation admits bright and dark solitonic solutions, depending on the sign of the interparticle interaction. The obstacle is modeled via an external potential, and this could correspond to different physical realizations, such as a heavy impurity, a (red or blue) detuned laser beam crossing the atomic beam, a bend, a twist, or a constriction in the shape of the guide.

A soliton under the influence of a perturbation (here, the obstacle) sees its shape and velocity modified and may also radiate energy (see, e.g., Ref. [8]). Despite their mutual dependence, these two phenomena are not easily treated on the same theoretical footing. The evolution of the soliton's parameters is typically studied within the adiabatic approximation (see Ref. [9] and references therein), whereas radiative effects are not so easily described, because their influence on the soliton's parameters only appears at second order in perturbation theory (see the discussion in Section 4.4). However, it has been possible to treat both phenomena concomitantly in the case of bright solitons [8–12]. Concerning dark solitons, several studies of adiabatic dynamics have appeared [13–19], but until recently radiative effects have been treated mainly numerically [20–22].

In the present paper we study the dynamics of a dark soliton via perturbation theory. This method, based on the theory of linear partial differential equations, has been established in the case of the nonlinear Schrödinger equation with repulsive interaction in Refs. [23,24] (see also the earlier attempt [25]). Although our first interest lies in the physics of guided Bose-Einstein condensates, the method employed and the results displayed also apply to optical waveguides described by a one-dimensional (1D) nonlinear defocussing Schrödinger equation.

The paper is organized as follows. In Section 2 we present the basic ingredients of the model and the resulting equation governing the time evolution of the condensate wave function. In the framework of perturbation theory we then derive the equations determining the dynamics of the soliton and of the radiated part (Section 3). The results are analysed in Section 4. We show that one can devise a quite successful approximation that we denote as “effective potential theory,” where the soliton is assimilated to a classical particle of mass twice the mass of a bare particle, evolving in an effective potential (Section 4.1). The agreement of this approximation with the results of the adiabatic approximation is verified even for a fine quantity such as the position shift induced on the trajectory of the soliton by the obstacle (Section 4.2). We then consider in Section 4.3 the radiated part and show that it is formed of backward- and forward-emitted phonons, which form two counterpropagating wavepackets moving at the speed of sound. In the limit of large soliton’s velocity we furthermore obtain in Section 4.4 an analytical expression for the total amount of radiation emitted by the soliton during the collision. In addition we show that (within our leading-order evaluation) a soliton reaching the velocity of sound does not radiate, and we propose a physical interpretation for this phenomenon. Finally we present our conclusions in Section 5. Some technical points are given in the Appendixes. In Appendix A we recall the main properties of the spectrum of the operator governing the wave dynamics of the system around the solitonic solution. In Appendix B we briefly present the Lagrangian approach for deriving the dynamics of the parameters of a dark soliton. In Appendix C we show how to compute some integrals involved in the evaluation of the total amount of radiation emitted by the soliton.

2 The model

We consider a condensate confined in a guide of axis z and denote by $n(z, t)$ the 1D density of the system. The condensate is formed by atoms of mass m which interact via a two-body potential characterized by its 3D s-wave scattering length a_{sc} . We consider the case of a repulsive effective interaction-i.e., $a_{sc} > 0$. The condensate is confined in the transverse direction by an harmonic potential of pulsation ω_{\perp} . The transverse confinement is characterized by the harmonic oscillator length $a_{\perp} = (\hbar/m\omega_{\perp})^{1/2}$.

With n_{1D} denoting a typical order of magnitude of $n(z, t)$, we restrict ourselves to a density range such that

$$(a_{sc}/a_{\perp})^2 \ll n_{1D} a_{sc} \ll 1. \quad (1)$$

This regime has been called “1D mean field” in Ref. [26]. In this range the wave function of the condensate can be factorized in a transverse and longitudinal part [27–29]. The transverse wave function is Gaussian (this is ensured by the condition $n_{1D} a_{sc} \ll 1$) and the longitudinal one, denoted by $\psi(z, t)$ [such that $n(z, t) = |\psi(z, t)|^2$], satisfies an effective 1D Gross-Pitaevskii equation (see, e.g., [27–29]):

$$-\frac{\hbar^2}{2m}\psi_{zz} + \left\{ U(z) + 2\hbar\omega_{\perp} a_{sc} |\psi|^2 \right\} \psi = i\hbar \psi_t. \quad (2)$$

In Eq. (2), $U(z)$ represents the effect of the obstacle. We restrict ourselves to the case of localized obstacle such that $\lim_{z \rightarrow \pm\infty} U(z) = 0$. Hence, we can consider that the stationary solutions of

Eq.(2) have at infinity an asymptotic density unperturbed by the obstacle. Besides, considering solutions without current at infinity, we impose the following form to the stationary solutions:

$$\psi_{\text{sta}}(z, t) = f(z) \exp[-i\mu t/\hbar], \quad \text{with} \quad \lim_{z \rightarrow \pm\infty} f(z) = \sqrt{n_\infty}, \quad (3)$$

where n_∞ is the 1D density far from the obstacle and $\mu = 2\hbar\omega_\perp a_{sc}n_\infty$ the chemical potential [30].

We note here that in Eq.(1) we have discarded very low densities in order to prevent the system from getting in the Tonks-Girardeau regime where the mean-field picture implicit in Eq. (2) breaks down [28, 31]. This can be intuitively understood as follows: it is natural to assume that the Gross-Pitaevskii scheme is valid-i.e., that the system can be described by a collective order parameter ψ -only if the interparticle distance (of order n_∞^{-1}) is much smaller than the minimum distance ξ over which ψ can significantly vary [ξ is the healing length, defined by $\xi = \hbar/(m\mu)^{1/2} = a_\perp/(2a_{sc}n_\infty)^{1/2}$]. The condition $n_\infty^{-1} \ll \xi$ then imposes us to consider the regime $n_\infty a_{sc} \gg (a_{sc}/a_\perp)^2$ to which, from Eq. (1), we restrict our study. If one considers, for instance, ^{87}Rb or ^{23}Na atoms in a guide with a transverse confinement characterized by $\omega_\perp = 2\pi \times 500$ Hz, the ratio a_{sc}/a_\perp is roughly of order 10^{-2} and the restriction (1) still allows the density to vary over four orders of magnitude.

In all the following we use dimensionless quantities: the energies are expressed in units of μ , the lengths in units of ξ , and the time in units of \hbar/μ . ψ is also rescaled by a factor $n_\infty^{-1/2}$; this corresponds to expressing the linear density in units of the density at infinity, n_∞ . We keep the same notation z , t , $U(z)$, and $\psi(z, t)$ for the rescaled quantities. Equation (2) now reads

$$-\frac{1}{2}\psi_{zz} + \{U(z) + |\psi|^2\}\psi = i\psi_t. \quad (4)$$

From Eq.(3), the stationary solutions of Eq.(4) are of type $f(z)\exp[-it]$, f being real, and a solution of

$$-\frac{1}{2}f_{zz} + \{U(z) + f^2 - 1\}f = 0, \quad (5)$$

with the asymptotic condition $\lim_{z \rightarrow \pm\infty} f(z) = 1$.

The method we will expose is quite general and applies to a broad range of potentials $U(z)$, but for concreteness we will often display the explicit solutions of the problem in the case of a pointlike obstacle, where $U(z) = \lambda\delta(z)$; $\lambda > 0$ (< 0) corresponds to a repulsive (attractive) obstacle. For such an obstacle, the solution of Eq.(5) is

$$f(z) = \begin{cases} \tanh(|z| + a) & \text{if } \lambda > 0 \\ \coth(|z| + a) & \text{if } \lambda < 0 \end{cases} \quad \text{with} \quad a = \frac{1}{2} \sinh^{-1} \left(\frac{2}{|\lambda|} \right). \quad (6)$$

In section 4 we will concentrate on perturbative aspects of the problem and consider the case of a weak potential $U(z)$. For a pointlike obstacle, this corresponds to the limit $|\lambda| \ll 1$. In this case $\sinh^{-1}(2/|\lambda|) \simeq \ln(4/|\lambda|)$ and Eqs. (6) simplify to

$$f(z) \simeq 1 - \frac{\lambda}{2} \exp\{-2|z|\}. \quad (7)$$

In the general case, one can design a simple treatment [29, 32] valid for any weak potential $U(z)$ leading after linearization of Eq. (5) to the perturbative result $f(z) = 1 + \delta f(z)$ with

$$\delta f(z) \simeq -\frac{1}{2} \int_{-\infty}^{+\infty} dy U(y) \exp\{-2|z - y|\}, \quad (8)$$

of which Eq.(7) is a particular case. In section 4 it will reveal convenient to rewrite Eq.(8) in an other way: denoting by $\hat{U}(q) = \int_{\mathbb{R}} dz U(z) \exp(-iqz)$ the Fourier transform of $U(z)$, one may equivalently express δf defined in Eq.(8) as

$$\delta f(z) \simeq -2 \int_{-\infty}^{+\infty} \frac{dq}{2\pi} \frac{\hat{U}(q)}{4 + q^2} \exp\{iqz\}. \quad (9)$$

The stationary solutions of the problem being defined, let us now turn to the main subject of the present work and consider the case of time-dependent solutions corresponding to a dark soliton propagating in the system. The soliton will appear as a distortion of the stationary background, and it is here very natural to follow the approach of Frantzeskakis *et al.* [17] who write the wave function of the system as a product:

$$\psi(z, t) = \phi(z, t) f(z) \exp(-it). \quad (10)$$

$\phi(z, t)$ in Eq. (10) accounts for the deformation of the stationary background $f(z) \exp(-it)$ caused by the motion of a soliton in the system. From Eq. (4) we see that the unknown field $\phi(z, t)$ is a solution of the following equation:

$$i\phi_t + \frac{1}{2}\phi_{zz} - \left\{|\phi|^2 - 1\right\}\phi = R[\phi], \quad (11)$$

where

$$R[\phi] = -\phi_z \frac{f_z}{f} + (f^2 - 1)(|\phi|^2 - 1)\phi. \quad (12)$$

Far from the obstacle, $f(z) = 1$ and thus $R[\phi] = 0$. In this case, the motion of a dark soliton in the system is described by the usual solitonic solution of the defocussing nonlinear Schrödinger equation [33]

$$\phi(z, t) = \Phi(z - Vt - b, \theta), \quad (13)$$

where

$$\Phi(x, \theta) = \chi(x, \theta) + iV, \quad \text{with} \quad \chi(x, \theta) = \cos \theta \tanh(x \cos \theta) \quad \text{and} \quad \sin \theta = V. \quad (14)$$

Equations (13) and (14) describe a dark soliton consisting in a density trough located at position $Vt + b$ at time t . The phase change across the soliton is $2\theta - \pi$. The choice of the parameter θ in $[0, \pi/2]$ corresponds to a soliton moving from left to right with a velocity $V = \sin \theta \in [0, 1]$. Note that a dark soliton has a velocity always lower than unity (which, in our rescaled units, is the velocity of sound [34]). When $\theta = 0$, the soliton is standing and its minimum density is zero;

it is referred to as a black soliton. When $\theta \neq 0$ one speaks of a gray soliton. We display in Fig. 1 the density profile and the phase of the wave function $\psi(z, t)$ [see Eq. (10)] describing a soliton incident with velocity $V = 0.4$ on a repulsive point-like obstacle characterized by $\lambda = 0.5$.

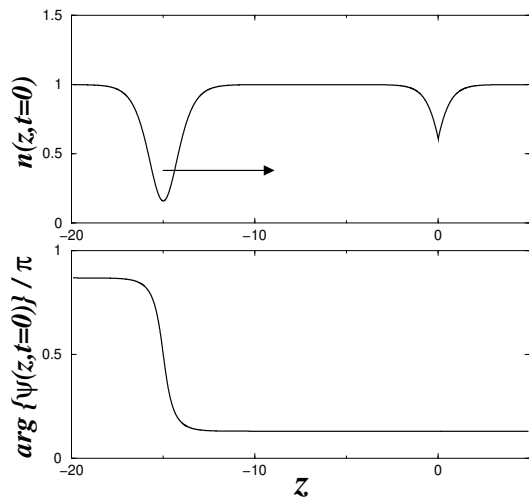


Figure 1: *Upper plot: density profile of a dark soliton incident with velocity $V = 0.4$ on a point-like repulsive obstacle $U(z) = \lambda \delta(z)$ (with $\lambda = 0.5$). The arrow represents the direction of propagation of the soliton. Lower plot: phase of the wave function $\psi(z, t = 0)$ describing the system. Across the soliton the phase of the wave function changes from $\pi - \theta$ to θ (with $V = \sin \theta$).*

3 Perturbation theory

In the following we will set up the basis for a systematic perturbative expansion, and for properly identifying the orders of perturbation at which the expansion is done, it is customary to introduce an artificial multiplicative parameter ϵ in the potential of the obstacle (otherwise of arbitrary form). We will see in the present section (and justify on physical grounds in the next one) that for an obstacle characterized by $\epsilon U(z)$, the condition of small perturbation reads $V^2 \gg \epsilon U$. Since the soliton velocity is always lower than unity (which is the speed of sound in our dimensionless units), this condition implies $\epsilon U \ll 1$; i.e., Eqs. (8,9) hold.

At initial times the soliton is unperturbed and described as in the previous section by $\phi(z, t) = \Phi(z - Vt, \theta_0)$ [Φ is defined in Eq. (14)]; i.e., one considers a soliton incident from left infinity with velocity $V = \sin \theta_0$. The more important effect of the obstacle on the soliton is a modification of its shape; i.e., the parameters characterizing the soliton will become time dependent in the vicinity of the obstacle. Perturbation at next order describe the emission of radiations. One thus looks for solutions of Eq.(11) of the form

$$\phi(z, t) = \phi_{\text{sol}}(z, \bar{z}(t), \theta(t)) + \delta\phi(z, t), \quad (15)$$

where

$$\phi_{\text{sol}}(z, \bar{z}(t), \theta(t)) = \Phi(z - \bar{z}(t), \theta(t)), \quad (16)$$

describes a soliton which is characterized by the two parameters $\bar{z}(t)$ (describing the center of the soliton) and $\theta(t)$ (describing the phase shift across the soliton). $\delta\phi$ describes additional radiative components:

$$\delta\phi(z, t) = \epsilon \phi_1(z, t) + \epsilon^2 \phi_2(z, t) + \dots \quad (17)$$

Equations (15)-(17) form the grounds of a secular perturbation theory where the time dependence of the parameters of the soliton permits to avoid the grow of secular perturbation in $\delta\phi$ (see, e.g., the discussion in Ref. [8]).

It is more appropriate to define $\delta\phi$ in Eq.(15) and the ϕ_i 's in Eq.(17) as functions of $z - \bar{z}(t)$ than as functions of z . To this end, we define $x = z - \bar{z}(t)$ and choose to work with x and t as independent parameters rather than z and t . This corresponds to the transformation

$$\partial_z, \partial_t \rightarrow \partial_x, \partial_t - \dot{\bar{z}} \partial_x. \quad (18)$$

Furthermore, in order to take into account the slow time dependence of the parameters of the soliton, it is customary to introduce multiple time scales: $t_n = \epsilon^n t$ ($n \in \mathbb{N}$). A time-dependent function could, for instance, depend on t via t_1 , indicating a weak time dependence (a t_2 dependence being related to an even weaker time dependence and a t_0 dependence to a ‘‘normal’’ time dependence). Generically, time-dependent quantities will be considered as functions of all the t_n 's, with

$$\partial_t = \partial_{t_0} + \epsilon \partial_{t_1} + \epsilon^2 \partial_{t_2} + \dots. \quad (19)$$

In the following we will make an expansion at order ϵ and it will suffice to consider only the fast time t_0 and the first slow time t_1 . The soliton's parameters θ and \bar{z} are considered as functions $\theta(t_1)$ and $\bar{z}(t_0, t_1)$ [35].

Putting everything together, we see that, at order ϵ , Eqs. (15)-(17) read explicitly

$$\phi(z, t) = \Phi(x, \theta(t_1)) + \epsilon \phi_1(x, t_0, t_1), \quad \text{with } x = z - \bar{z}(t_0, t_1). \quad (20)$$

Equation(11) is now rewritten taking the transformations (18) and (19) into account, with an expansion at order ϵ . To this end, we have to take into account that $R[\phi]$ defined in Eq.(12) is a small quantity and can be written at first order in ϵ as

$$R[\phi] \simeq -\partial_x \Phi(x, \theta) [\partial_z \delta f(z) + 2 \Phi(x, \theta) \delta f(z)] \equiv \epsilon \mathcal{R}(x, z), \quad (21)$$

where $z = x + \bar{z}(t_0, t_1)$ and $\delta f(z)$ is defined as in Eqs.(8) and (9), with an extra multiplicative factor ϵ in U which has been written explicitly in the definition of \mathcal{R} on the right-hand-side (RHS) of Eq.(21).

We are now ready to expand Eq.(11) in successive orders in ϵ . The leading order reads

$$-\frac{1}{2} \Phi_{xx} + i \bar{z}_{t_0} \Phi_x + (|\Phi|^2 - 1) \Phi = 0, \quad (22)$$

implying that

$$\bar{z}_{t_0} = \sin \theta, \quad (23)$$

whence \bar{z} can be written as

$$\bar{z} = t_0 \sin \theta + \tilde{z}(t_1), \quad (24)$$

where $\tilde{z}(t_1)$ is a still unknown function [36]. At next order in ϵ one obtains

$$i \partial_{t_0} \phi_1 = \left[-\frac{1}{2} \partial_x^2 + i \sin \theta \partial_x + 2|\Phi|^2 - 1 \right] \phi_1 + \Phi^2 \phi_1^* + \mathcal{R} - i \theta_{t_1} \Phi_\theta + i \bar{z}_{t_1} \Phi_x. \quad (25)$$

Equation (25) can be rewritten as

$$i\partial_{t_0}|\phi_1\rangle = \mathcal{H}|\phi_1\rangle + \sigma_3|\mathcal{R}\rangle + i\bar{z}_{t_1}|\omega_e\rangle - \frac{\theta_{t_1}}{\cos\theta}|\Omega_e\rangle, \quad (26)$$

where $|\phi_1\rangle = (\phi_1, \phi_1^*)^T$, $|\mathcal{R}\rangle = (\mathcal{R}, \mathcal{R}^*)^T$, σ_3 is the third Pauli matrix, and

$$\mathcal{H} = \begin{pmatrix} -\frac{1}{2}\partial_x^2 + i\sin\theta\partial_x + 2|\Phi|^2 - 1 & \Phi^2 \\ -\Phi^{*2} & \frac{1}{2}\partial_x^2 + i\sin\theta\partial_x - 2|\Phi|^2 + 1 \end{pmatrix}. \quad (27)$$

\mathcal{H} is not diagonalizable, but can be put in a Jordan form in a manner similar to what has been done for the attractive nonlinear Schrödinger equation [37]. Its eigenfunctions and eigenvalues are presented in Appendix A. In particular, $|\omega_e\rangle$ and $|\Omega_e\rangle$ appearing in Eq.(26) belong to the generalized null space of \mathcal{H} ; they verify $\mathcal{H}|\omega_e\rangle = 0$ and $\mathcal{H}|\Omega_e\rangle = \cos^2\theta|\omega_e\rangle$. As well as its null space, \mathcal{H} has two continuous branches of excitations which we denote by its ‘‘phonon spectrum.’’ The corresponding eigenfunctions are denoted by $|\Xi_q^\pm\rangle$ with $q \in \mathbb{R}$ (see Appendix A).

It is physically intuitive that $|\phi_1\rangle$ corresponding to the radiated part should be expanded over the phonon part of the spectrum of \mathcal{H} :

$$|\phi_1\rangle = \sum_{\alpha=\pm} \int_{-\infty}^{+\infty} dq C_q^\alpha(t_0, t_1) |\Xi_q^\alpha\rangle. \quad (28)$$

A more technical argument for limiting the expansion (28) to the phonon components of the spectrum of \mathcal{H} is the following: one might think that a greater generality could be achieved by allowing $|\phi_1\rangle$ to have also components on $|\omega_e\rangle$ and $|\Omega_e\rangle$, for instance. However, exactly as in the case of the bright soliton [12], these components can (and should) be imposed to remain zero for avoiding the appearance of secular terms in the evolution of the soliton’s parameters.

3.1 Evolution of the parameters of the soliton

Applying $\langle\omega_e|\sigma_3$ and $\langle\Omega_e|\sigma_3$ onto (26) and using the orthogonality relations (A6), one obtains the equations of evolution of the parameters of the soliton:

$$\begin{aligned} 4\theta_{t_1}\cos^2\theta = -\langle\omega_e|\mathcal{R}\rangle &= -2\operatorname{Re}\left\{\int_{-\infty}^{+\infty} dx \Phi_x \mathcal{R}^*(x, x + \bar{z})\right\} \\ &= \frac{2}{\epsilon}\operatorname{Re}\left\{\int_{-\infty}^{+\infty} dz R^*[\phi_{\text{sol}}] \partial_z \phi_{\text{sol}}\right\}, \end{aligned} \quad (29)$$

and

$$\begin{aligned} 4\bar{z}_{t_1}\cos^2\theta = \frac{1}{i\cos\theta}\langle\Omega_e|\mathcal{R}\rangle &= -2\operatorname{Re}\left\{\int_{-\infty}^{+\infty} dx \Phi_\theta \mathcal{R}^*(x, x + \bar{z})\right\} \\ &= -\frac{2}{\epsilon}\operatorname{Re}\left\{\int_{-\infty}^{+\infty} dz R^*[\phi_{\text{sol}}] \partial_\theta \phi_{\text{sol}}\right\}. \end{aligned} \quad (30)$$

The set of equations (23),(29) and (30) describe the time evolution of the soliton’s parameter. The same equations are obtained via adiabatic approximation which is a simpler variational approximation where radiative effects are neglected [see Appendix B, Eqs. (B9) and (B10)]. This is

evident in the case of Eq. (29) which is the slow time analogous to Eq. (B9) (since $\dot{\theta} = \epsilon \theta_{t_1}$). In a similar way, the prescription (19) indicates that $\dot{\bar{z}} = \bar{z}_{t_0} + \epsilon \bar{z}_{t_1}$; combining Eqs. (23) and (30), one sees that the equations of evolution of \bar{z} obtained in the present section correspond to the multiple-time expansion of Eq.(B10). As a side result of this exact correspondance of the time evolution of the soliton's parameters, we obtain here that, as in the adiabatic approach, $\sin[\theta(t_1 \rightarrow \pm\infty)] = V$ (see the discussion at the end of Appendix B) and the quantity \bar{z} appearing in Eq. (24) is identical when $t_1 \rightarrow +\infty$ to the one defined in Eq. (48).

A technical remark is in order here. One can notice that in Eq.(15) we did not consider the most general variational form for the solitonic component of the wave function. We could have let its global phase depend on time, for instance, and this would have given in Eq.(26) a contribution along $|\omega_o\rangle$ ($|\omega_o\rangle$ is defined in Appendix A). Similarly, a more general variational ansatz could also have been used in Appendix B. The important point is that if the soliton's parameters are chosen within the same variational space, their time evolution is described – in the adiabatic and perturbative approach – by the same equations. Besides, the radiative term ϕ_1 having in all cases to be restricted to the phonon part of the spectrum, its time evolution is not (at least in the limit $V^2 \gg \epsilon U$; see below) affected by the specific choice of variational parameters used for describing the soliton.

3.2 Radiated part

The time evolution of the radiative component $|\phi_1\rangle$ is obtained in a manner similar to what is done for the soliton's parameters. Projecting Eq. (26) onto the phonon eigenfunctions of \mathcal{H} by applying $\langle \Xi_q^\alpha | \sigma_3$ yields

$$i \mathcal{N}_q^\alpha \partial_{t_0} C_q^\alpha = \mathcal{N}_q^\alpha \varepsilon_q^\alpha C_q^\alpha + \langle \Xi_q^\alpha | \mathcal{R} \rangle , \quad (31)$$

where $\alpha = \pm$. ε_q^α in Eq.(31) is the eigenvalue of \mathcal{H} associated with $|\Xi_q^\alpha\rangle$ [see Eq.(A2)]

$$\varepsilon_q^\alpha = q \left(-\sin \theta + \alpha \sqrt{\frac{q^2}{4} + 1} \right) , \quad (32)$$

and \mathcal{N}_q^α is a normalization factor [see Eqs.(A4) and (A5)]. In deriving Eq.(31), we have taken into account that the eigenfunctions $|\Xi_q^\alpha\rangle$ depend on t only through the slow time t_1 (via $\sin \theta$). The same holds for ε_q^α and \mathcal{N}_q^α . Thus, writing

$$C_q^\alpha(t_0, t_1) = D_q^\alpha(t_0, t_1) \exp\{-i \varepsilon_q^\alpha t_0\} , \quad (33)$$

one has, at the same order of approximation as Eq.(31),

$$\partial_{t_0} D_q^\alpha = \frac{1}{i \mathcal{N}_q^\alpha} \langle \Xi_q^\alpha | \mathcal{R} \rangle . \quad (34)$$

In integrating Eq. (34) we can choose between two equivalent strategies. The first (and difficult) one is to solve this equation taking into account that $t_1 = \epsilon t_0$ and that θ and \bar{z} have the time dependence specified by Eqs.(23),(29) and (30). The second one is to integrate this equation considering t_0 and

t_1 as independent variables. In this case, the t_1 dependence of θ and \bar{z} will not matter and the t_0 dependence of \bar{z} will be specified by Eq.(24). According to this second method one obtains

$$D_q^\alpha(t_0, t_1) = \frac{1}{i\mathcal{N}_q^\alpha} \int_{-\infty}^{t_0} dt'_0 e^{i\varepsilon_q^\alpha t'_0} \langle \Xi_q^\alpha | \mathcal{R} \rangle + \tilde{D}_q^\alpha(t_1), \quad (35)$$

where \tilde{D}_q^α is an unknown function of t_1 [verifying $\tilde{D}_q^\alpha(t_1 \rightarrow -\infty) = 0$] which could be determined by pushing the perturbative expansion to next order in ε . In the following we will simply neglect this term. This is legitimate in the limit where all the t_1 -dependent terms are nearly constant-i.e., to the limit where the parameters of the soliton are very weakly affected by the obstacle. We will see in the next section that this limit is reached when $\varepsilon U \ll V^2$.

Of most interest to us is the total amount of radiation emitted by the soliton. For the determination of this quantity we need the explicit expression of Eq.(35) at large times. In the limit t_0 and $t_1 \rightarrow +\infty$, Eq. (35) (without the \tilde{D}_q^α term) reads explicitly

$$D_q^\alpha(+\infty) = \frac{1}{i\mathcal{N}_q^\alpha} \int_{\mathbb{R}^2} dx dt'_0 e^{i\varepsilon_q^\alpha t'_0} \left[u_q^{\alpha*}(x) \mathcal{R}(x, x + \bar{z}(t'_0, +\infty)) + v_q^{\alpha*}(x) \mathcal{R}^*(x, \bar{z}(t'_0, +\infty)) \right], \quad (36)$$

where the functions $u_q^\alpha(x)$ and $v_q^\alpha(x)$ are the explicit components of $|\Xi_q^\alpha\rangle$ defined in Appendix A [Eq. (A3)]. Note that the t_1 -dependent parameters in Eq.(36) have been given their asymptotic value. In particular, $\sin\theta(t_1 \rightarrow +\infty) = \sin\theta_0 = V$, and according to Eq. (24) one has here $\bar{z}(t'_0, +\infty) = V t'_0 + \tilde{z}(+\infty)$. The integration along t'_0 in Eq.(36) can be computed easily using the expression (21) for \mathcal{R} and Eq.(9) for δf , leading to

$$D_q^\alpha(+\infty) = \frac{4}{iV\mathcal{N}_q^\alpha} \frac{\hat{U}^*\left(\frac{\varepsilon_q^\alpha}{V}\right)}{4 + \left(\frac{\varepsilon_q^\alpha}{V}\right)^2} e^{-i\varepsilon_q^\alpha \tilde{z}(+\infty)/V} \times \int_{\mathbb{R}} dx e^{-i\varepsilon_q^\alpha x/V} \partial_x \Phi \left[u_q^{\alpha*}(x) \left(\Phi(x) - \frac{i\varepsilon_q^\alpha}{2V} \right) + v_q^{\alpha*}(x) \left(\Phi(x)^* - \frac{i\varepsilon_q^\alpha}{2V} \right) \right]. \quad (37)$$

A long but straightforward computation gives the final result

$$D_q^\alpha(+\infty) = -\frac{1}{16V^3} \frac{q}{\sqrt{1+q^2/4}} \frac{\hat{U}^*(\varepsilon_q^\alpha/V) e^{-i\varepsilon_q^\alpha \tilde{z}(+\infty)/V}}{\sinh\left(\frac{\pi q \sqrt{1+q^2/4}}{2V \sqrt{1-V^2}}\right)}. \quad (38)$$

In this formula the term $\tilde{z}(+\infty)$ can be obtained through the numerical determination of $\bar{z}(t)$. We indicate in section 4.2 different approximation schemes allowing one to obtain an analytical evaluation of this term [Eq. (47) and below]. From expression (38) we see that the radiation contributes to (20) to the total wave function with a contribution of order $(\varepsilon \hat{U}/V^2) \sqrt{1-V^2}$. According to the approximation scheme defined in the beginning of the present section we have $V^2 \gg \varepsilon U$. Since \hat{U} and U are of same order of magnitude, the radiated part is, as expected, a small quantity.

4 Analysis of the results

In this section we analyse the solutions of Eqs (23),(29), and (30), (28),(33) and (34) which describe the dynamics of the system within our approach. The separation between the slow and fast times we used up to now in order to identify which time derivatives were negligible is no longer necessary, and we will henceforth only employ the actual time t . We will also drop the multiplicative factor ϵ in front of the perturbing potential $U(z)$ and of $\phi_1(x, t)$. In the two following subsections we study the evolution of the parameters of the soliton and in the two last ones we analyse the radiated part.

4.1 Effective potential approximation

Since we now use the actual time t , instead of using Eqs.(23),(29) and (30), it is more appropriate to work with the equivalent equations (B9,B10). In order to get insight into the details of the dynamics of the soliton, one should solve these equations numerically for a particular obstacle. This is done in section 4.2, where we study the behavior of a soliton incident on a delta scatterer. But before going to this point, it is interesting to study some limiting cases. In particular, the dynamics of the variational solution (16) can be more easily understood in the limit of a very dark soliton (almost back). To this end, let us multiply Eq. (B9) by $\dot{\bar{z}}$ and add it to Eq. (B10) multiplied by $\dot{\theta}$. This gives

$$4\dot{\theta} \sin \theta \cos^2 \theta = 2 \operatorname{Re} \left\{ \int_{-\infty}^{+\infty} dz R^*[\phi_{\text{sol}}] \left(\dot{\bar{z}} \partial_{\bar{z}} \phi_{\text{sol}} + \dot{\theta} \partial_{\theta} \phi_{\text{sol}} \right) \right\}. \quad (39)$$

In the limit of a weak potential, we have to keep in mind that R is a small quantity (of order of U). It is then legitimate at first order to replace on the RHS of (39) $\dot{\bar{z}}$ by $\sin \theta$ and to drop the term $\dot{\theta}$. One thus obtains

$$\dot{\theta} = \frac{3}{4} \cos^2 \theta \int_{-\infty}^{+\infty} dz \frac{\partial_z f}{\cosh^4[\cos \theta(z - \bar{z})]}. \quad (40)$$

A further simplification of the equations is obtained in the limit of very dark soliton, when $\theta \rightarrow 0$. In this limit $\dot{\theta} \simeq \dot{\bar{z}}$ and using expression (8) for f we can put Eq. (40) in the following form:

$$2\ddot{\bar{z}} = -\frac{dU_{\text{eff}}}{d\bar{z}} \quad \text{where} \quad U_{\text{eff}}(\bar{z}) = -\frac{3}{2} \int_{-\infty}^{+\infty} dz \frac{\delta f(z)}{\cosh^4(z - \bar{z})} = \frac{1}{2} \int_{-\infty}^{+\infty} dz \frac{U(z)}{\cosh^2(z - \bar{z})}. \quad (41)$$

If we furthermore consider a potential $U(z)$ which slowly depends on z (over a length scale much larger than unity [38]), then $U(z)$ in the convolution of the RHS of Eq.(41) does not appreciably vary over the distance where the term $\cosh^{-2}(z - \bar{z})$ is noticeable. This yields

$$U_{\text{eff}}(\bar{z}) \simeq \frac{U(\bar{z})}{2} \int_{-\infty}^{+\infty} dz \frac{1}{\cosh^2(z - \bar{z})} = U(\bar{z}). \quad (42)$$

Equations(41) and (42) show than in the appropriate limit (very dark soliton, weak and slowly varying potential) the soliton can be considered as an effective classical particle of mass 2 (i.e., twice the mass of a bare particle) of position \bar{z} (the position of the center of the density trough) evolving in a potential $U(\bar{z})$. If we relax the hypothesis of slowly varying potential, the soliton

can still be considered as a particle of mass 2, but it now evolves in an effective potential $U_{\text{eff}}(\bar{z})$ defined in Eq.(41) as a convolution of the real potential $U(z)$. The fact that the effective mass of the soliton is twice the one of a bare particle has already been obtained in Refs. [16, 17, 19, 39]. Previous studies mainly focused on slowly varying external potentials and, as a result, the existence of an effective potential U_{eff} – different from U – had not been noticed so far, except in Ref. [17] where this result has already been obtained in the special case of a δ scatterer. In the following, we denote the approximation corresponding to Eq. (41) as the effective potential approximation: the soliton is considered as an effective classical particle of mass 2, position \bar{z} , moving in the potential $U_{\text{eff}}(\bar{z})$.

4.2 Numerical check

Let us now study in detail a particular example. We consider a soliton incident on a pointlike obstacle-i.e., a δ scatterer characterized by $U(x) = \lambda \delta(x)$. In this case, the static background $f(z)$ is given by Eq(6) and Eqs. (B9) and (B10) read

$$\begin{aligned} \dot{\theta} = & \text{sgn}(\lambda) \cos^2 \theta \int_0^{+\infty} \frac{dz}{\sinh(2z + 2a)} \left(\frac{1}{\cosh^4 X} - \frac{1}{\cosh^4 Y} \right) \\ & + \frac{\cos^3 \theta}{2} \int_0^{+\infty} dz [1 - f^2(z)] \left(\frac{\tanh X}{\cosh^4 X} - \frac{\tanh Y}{\cosh^4 Y} \right), \end{aligned} \quad (43)$$

and

$$\begin{aligned} \sin \theta - \dot{\bar{z}} = & \text{sgn}(\lambda) \sin \theta \int_0^{+\infty} \frac{dz}{\sinh(2z + 2a)} \left(\frac{X \cosh^{-2} X + \tanh X}{\cosh^2 X} + \frac{Y \cosh^{-2} Y + \tanh Y}{\cosh^2 Y} \right) \\ & + \frac{\sin \theta \cos \theta}{2} \int_0^{+\infty} dz [1 - f^2(z)] \left(\frac{1 - X \tanh X}{\cosh^4 X} + \frac{1 - Y \tanh Y}{\cosh^4 Y} \right). \end{aligned} \quad (44)$$

X and Y in Eqs. (43) and (44) are notations for $(z - \bar{z}) \cos \theta$ and $(z + \bar{z}) \cos \theta$ respectively, and the expressions of function f and of parameter a are given in Eq. (6). Solving Eqs. (43) and (44) numerically, we obtain the time evolution of the parameters of the soliton. We plot in Figs. 2 and 3 the behavior of \bar{z} as a function of t for different initial velocities V . Figure 2 corresponds to a repulsive interaction with $\lambda = +1$ and Fig. 3 to an attractive one with $\lambda = -1$. The initial conditions for the numerical integration of Eqs. (43) and (44) are taken to be $\bar{z}(t = 0) = -10$ and $\dot{\bar{z}}(t = 0) = \sin[\theta(t = 0)] = V$. Several curves are drawn, corresponding to several values of V . In the repulsive case (Fig. 2), three initial velocities have been chosen: $V = 0.9$, 0.707 , and 0.4 . The value $V = 0.9$ corresponds to a fast soliton which is weakly perturbed by the barrier, the value $V = 0.4$ corresponds to a reflected soliton, and the value $V = 0.707$ is just below the value $V = \sqrt{\lambda/2}$ which, according to the effective potential approximation (41), is the separatrix between transmission and reflexion (corresponding to $V^2 = \max \{U_{\text{eff}}(\bar{z})\} = \lambda/2$). In the attractive case (Fig. 3) the curves are drawn in the cases $V = 0.707$, 0.4 and 0.3 . In both figures, the solid lines correspond to the exact numerical solution of Eqs.(43) and (44) and the dashed lines to the result of the effective potential approximation.

We first remark that the case of a δ scatterer we consider here is the worst possible for the effective potential approximation and that this approximation is certainly more at ease with smoother

potentials. However, it is interesting to note that the effective potential approximation, which could be thought as oversimplified, is often very good. The worst agreement occurs in the case of repulsive obstacle, near the separatrix (which is estimated by the effective potential approximation to occur in the case of Fig. 2 at $V = 1/\sqrt{2}$). As we will see below (Fig. 4), the effective potential approximation does not exactly predict the location of this separatrix whereas, in this region, the trajectories are strongly affected by small changes of the initial velocity V . This is the reason for the bad agreement of the result of the approximate method with the ones given by the numerical integration of Eqs. (43) and (44) for $V = 0.707$. However, it is surprising to note that the effective potential approximation is generically valid, even in the case where the soliton is far from being very dark: even the limit $V \rightarrow 1$ is very accurately described by this approximation on Figs. 2 and 3.

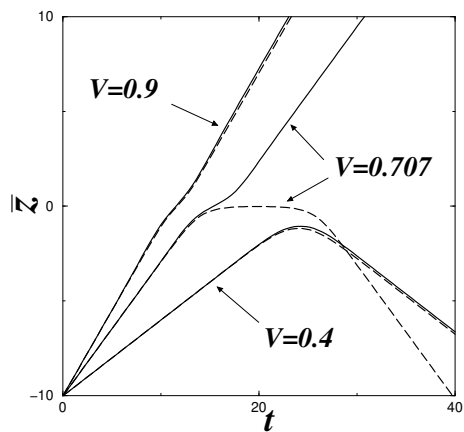


FIG. 2. $\bar{z}(t)$ for solitons of initial velocity V , incident on a repulsive obstacle $U(x) = \lambda \delta(x)$ with $\lambda = +1$. The solid lines correspond to the numerical solution of Eqs.(43) and (44) and the dashed lines to the effective potential approximation (41).

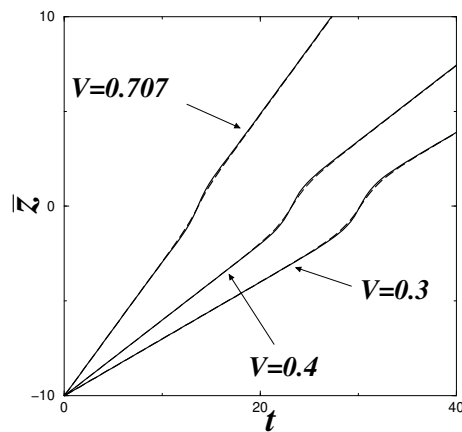


FIG. 3.: Same as Fig. 2 for solitons incident on an attractive obstacle $U(x) = \lambda \delta(x)$ with $\lambda = -1$. The dashed lines corresponding to the effective potential approximation are hardly distinguishable from the solid lines which correspond to the numerical solution of Eqs.(43) and (44).

In order to investigate more precisely the limit of large initial velocities V and to assess the validity of the effective potential approximation, let us now establish the form of Eqs. (B9) and (B10) in the case of a weakly perturbed soliton. From the effective potential approximation, one infers that the soliton is weakly perturbed by the obstacle when its initial energy is large compared to the external potential U_{eff} i.e., in the regime $V^2 \gg U$ (since U_{eff} and U are typically of same order of magnitude). This is confirmed by the numerical results presented on Figs. 2 and 3: the trajectory of the soliton is less modified for large V . In the extreme limit $V^2 \gg U$ one may write $\theta(t) = \theta_0 + \Theta(t)$ and $\bar{z} = Vt + \Delta(t)$, with $\Theta \ll \theta_0$ and $\dot{\Delta} \ll V$. Δ has the meaning of a shift in position: it is the difference between the position of the center of the soliton in presence of the obstacle with the value it would have in absence of the obstacle. The perturbative versions of Eqs.

(B9) and (B10) read

$$4 \dot{\Theta} \cos^2 \theta_0 = -2 \operatorname{Re} \int_{-\infty}^{+\infty} dz R^* [\Phi(z - Vt, \theta_0)] \Phi_z(z - Vt, \theta_0) \quad (45)$$

and

$$4 \cos^2 \theta_0 [\Theta \cos \theta_0 - \dot{\Delta}] = 2 \operatorname{Re} \int_{-\infty}^{+\infty} dz R^* [\Phi(z - Vt, \theta_0)] \Phi_\theta(z - Vt, \theta_0). \quad (46)$$

From these equations it is a simple matter to compute analytically the asymptotic expressions of the soliton parameter. One obtains – as expected – $\Theta(+\infty) = 0$, and the asymptotic shift in position is

$$\Delta(+\infty) = -\hat{U}(0) \frac{1 + 2V^2}{6V^2}, \quad (47)$$

where $\hat{U}(0) = \int_{\mathbb{R}} dx U(x)$. Equation (47) for $\Delta(+\infty)$ is an approximation (valid in the regime $V^2 \gg U$) of the exact result

$$\Delta(+\infty) = \lim_{t \rightarrow +\infty} \{\bar{z}(t) - Vt\}. \quad (48)$$

Comparing definitions (24) and (48) we see that, since $\sin \theta(t_1 \rightarrow +\infty) = V$, one has $\Delta(+\infty) = \bar{z}(+\infty)$. In the case of a δ scatterer, the exact value (48) was computed through numerical solution of Eqs. (43) and (44). The result is displayed in Fig. 4 (thick solid curves) and compared with the approximate expression (47) (thin solid curves) and with the result of the effective potential approximation (dashed curves).

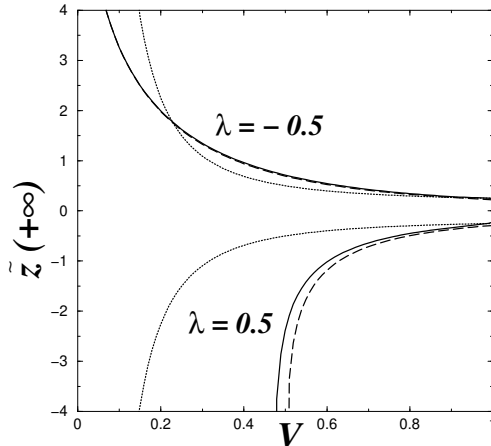


FIG. 4. $\Delta(+\infty)$ as a function of the initial velocity V of a soliton incident on a δ peak $U(x) = \lambda \delta(x)$. The upper curves correspond to the case $\lambda = -0.5$, the lower ones to the case $\lambda = 0.5$. The thick solid lines are the exact result (48) obtained from the numerical integration of Eqs. (43) and (44). The dashed curves are the result (49) of the effective potential approximation and the thin solid curves are the approximate result (47).

In the case of the effective potential approximation, the value of the shift $\Delta(+\infty)$ can be computed either via the numerical solution of the equation of motion (41) or via the formula

$$\Delta(+\infty) = \int_{-\infty}^{+\infty} dx \left[1 - \frac{1}{\sqrt{1 - U_{\text{eff}}(x)/V^2}} \right]. \quad (49)$$

From this expression, one sees that in the limit $V^2 \gg U_{\text{eff}} \sim U$, the effective potential approximation yields a result $\Delta(+\infty) \simeq -\frac{1}{2} \hat{U}(0)/V^2$. Hence, in this limit, the shift computed via the effective potential approximation at $V = 1$ is correct [since it agrees with the result (47) at $V = 1$]. This is surprising, because the effective potential approximation is expected to be accurate only for very dark solitons. However, one can also notice that detailed agreement with the exact result (48) is missed since, in the limit $V^2 \gg U$, the asymptotic evaluation (47) of (48) does not exactly match the one of (49). Yet one sees from Fig. 4 that the shift computed via the effective potential approximation is in surprisingly good agreement with the exact value, even for fast solitons. In particular, in the case of an attractive potential, the exact evaluation of $\Delta(+\infty)$ and its approximation (49) are hardly distinguishable.

4.3 Backward- and forward- emitted wave packets

At this point it is interesting to study in more detail the structure of the phonon part of the wave function-i.e., of $\phi_1(x, t)$. From Eqs. (28) and (A3) one can separate ϕ_1 into two parts: $\phi_1 = \phi_1^+ + \phi_1^-$ with

$$\phi_1^\alpha(x, t) = \int_{\mathbb{R}} dq C_q^\alpha(t) u_q^\alpha(x). \quad (50)$$

From the explicit expressions (32), (33) and (A3) one sees that ϕ_1^+ (ϕ_1^-) describes waves propagating toward the positive (negative) x .

We are interested in studying the outcome of the collision-i.e., in obtaining an analytical evaluation of Eq(50) when $t \rightarrow +\infty$. To this end, one uses the fact that at large time one has $C_q^\alpha(t) \propto \exp\{-i\varepsilon_q^\alpha[t + \tilde{z}(+\infty)/V]\}$. Hence, instead of working with the variable t , it is convenient here to define $\tau = t + \tilde{z}(+\infty)/V$ and to write Eq. (50) in the form

$$\phi_1^\alpha(x, t) = \int_{\mathbb{R}} dq G^\alpha(q, x) \exp\{i[q(x + V \tau) - \alpha \tau F(q)]\}, \quad (51)$$

where $F(q) = q(q^2/4 + 1)^{1/2}$ and $G^\alpha(q, x) = [q/2 + \varepsilon_q^\alpha/q + i\chi(x)]^2 D_q^\alpha(+\infty) \exp\{i\varepsilon_q^\alpha \tilde{z}(+\infty)/V\}$. In the appropriate limit (to be defined soon), one can evaluate this expression through a saddle phase estimate. In this limit, the rapidly oscillating phase in Eq.(51) is stationary at point $\pm q_\alpha$ which are solutions of $x + V \tau = \alpha \tau F'(q)$. One has

$$q_\alpha^2 = \frac{1}{2} \left[X^2 - 4 + \alpha X \sqrt{X^2 + 8} \right], \quad \text{with} \quad X = V + \frac{x}{\tau}. \quad (52)$$

One can easily verify that q_α goes to zero when $V + \frac{x}{\tau} = \alpha$ and that q_α^2 is positive only if $\alpha(V + \frac{x}{\tau}) > 1$. From this, one sees that the saddle phase estimate of Eqs.(50) and (51) is accurate when the two saddles are well separated-i.e., in the regime $x \gg (1 - V) \tau$ for $\alpha = +$ and $x \ll -(1 + V) \tau$ for $\alpha = -$. If this condition is fulfilled, one obtains

$$\begin{aligned} \phi_1^\alpha(x, t) &\simeq G^\alpha(q_\alpha, x) \sqrt{\frac{2\pi}{|F''(q_\alpha)|}} e^{i[q_\alpha(x+V\tau) - \alpha\tau F(q_\alpha) - \alpha\pi/4]} \\ &+ G^\alpha(-q_\alpha, x) \sqrt{\frac{2\pi}{|F''(q_\alpha)|}} e^{-i[q_\alpha(x+V\tau) - \alpha\tau F(q_\alpha) - \alpha\pi/4]}. \end{aligned} \quad (53)$$

The exact expression computed from Eq.(50) is compared in Fig. 5 with the saddle phase estimate (53). The curves are drawn at $\tau = 60$ [40] for a soliton with incident velocity $V = 0.5$. The obstacle is here taken to be a delta scatterer $\lambda \delta(x)$. ϕ_1 being proportional to λ [through the expression (38) of $D_q^\alpha(+\infty)$] we represent in Fig. 5 the value of $\phi_1(x, t)/\lambda$ (actually its real part) which do not depend on λ .

One sees in Figure 5 that the semiclassical approximation (53) is excellent in all its expected domain of validity and diverges at $x = (1 - V)\tau = 30$ (for $\alpha = +$) and $x = -(1 + V)\tau = -90$ (for $\alpha = -$) [41]. Hence, these points can be considered as representative of the region where the contribution of ϕ_1^+ and ϕ_1^- to the total wave function is more important. Roughly speaking, the present approach indicates that, long after the collision, $\phi_1^\alpha(x, t)$ is maximum around $x = (\alpha - V)\tau$. We recall that when using x (instead of z) as position coordinate, the soliton is, at all times, located around $x = 0$. Hence, going back to the z coordinate, we have a clear picture of the process at large times: the soliton propagates at velocity V (the same as its initial velocity) after having emitted phonons which form two wave packets, one propagating in the forward direction with group velocity 1 (i.e., the sound velocity) and the other one propagating backwards with group velocity -1 . The same conclusion seems to be reached in the numerical simulations of Parker *et al.* [21, 22].

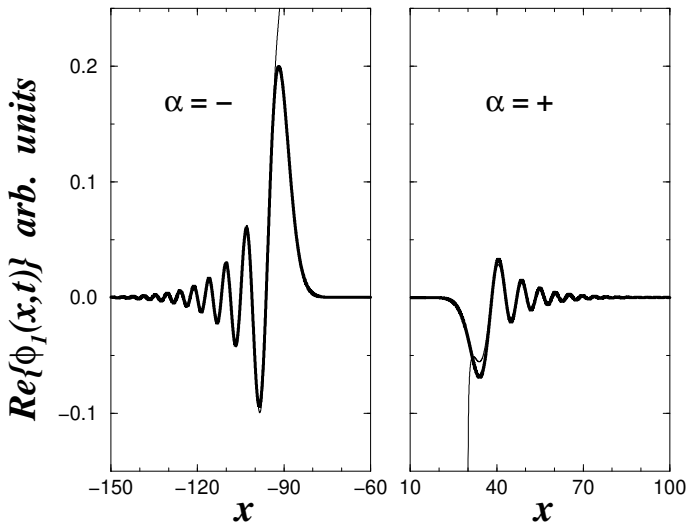


Fig. 5. $Re\{\phi_1(x, t)\}$ as a function of x for $\tau = 60$ for a soliton of initial velocity $V = 0.5$ incident on a δ scatterer $\lambda \delta(x)$. The thick line represents the result (50) and the thin line its semiclassical approximation (53). For legibility we have separated the region where ϕ_1^- is nonzero (around $x = -90$) from the one where ϕ_1^+ is non zero (around $x = 30$). Note that in the expected domain of validity of Eq. (53) ($x \gg 30$ and $x \ll -90$) one can hardly distinguish the thick line from its semiclassical approximation.

4.4 Radiated energy

A quantity of importance for characterizing the system is the total energy radiated by the soliton. Equation(4) for the field ψ which, in the present work, is of the form $\varphi(z, t) \exp(-it)$ [cf. Eq. (10)], conserves the energy \mathcal{E} defined as:

$$\mathcal{E}[\varphi] = \int_{\mathbb{R}} dz \left\{ \frac{1}{2} |\varphi_z|^2 + \frac{1}{2} (|\varphi|^2 - 1)^2 + U(z) |\varphi|^2 \right\}. \quad (54)$$

In order to have an expression of the energy in terms of the field ϕ which, when $\phi = \Phi$, matches the usual expression (B3) of the energy of the soliton, we rather work with the quantity $E[\phi] = \mathcal{E}[f\phi] - \mathcal{E}[f]$. $E[\phi]$ is of course a conserved quantity, and we are interested in its expression far

before ($t \rightarrow -\infty$) and far after ($t \rightarrow +\infty$) the collision with the obstacle. We note here that $f(z) - 1$ and $U(z)$ are non zero only when z is close to origin, whereas, in the same region, $\phi(z, t) - 1$ is zero when $t \rightarrow \pm\infty$. After a change of variable from z to $x = z - \bar{z}(t)$, the previous remark allows one to obtain the simplified expression for E (only valid when $t \rightarrow \pm\infty$):

$$E[\phi] = \frac{1}{2} \int_{\mathbb{R}} dx \{ |\phi_x|^2 + (|\phi|^2 - 1)^2 \} . \quad (55)$$

Using the decomposition (15), keeping the lowest orders in $\delta\phi$, and taking into account the fact that, when $t \rightarrow \pm\infty$, $|\Phi|^2 - 1$ is zero in the regions where $\delta\phi$ is noticeable, one obtains

$$E[\phi] = \frac{1}{2} \int_{\mathbb{R}} dx \{ |\Phi_x|^2 + (|\Phi|^2 - 1)^2 \} + \frac{1}{2} \int_{\mathbb{R}} dx \left\{ |\delta\phi_x|^2 + (\Phi^* \delta\phi + \delta\phi^* \Phi)^2 \right\} + \mathcal{O}(\delta\phi^3) . \quad (56)$$

The first integral on the RHS of Eq.(56) corresponds to the soliton's energy and is equal to $\frac{4}{3} \cos^3 \theta$. The second integral on the RHS of Eq.(56) corresponds to the energy of the radiated part and is denoted by E_{rad} in the following.

We are now facing a difficulty: we performed a computation at order ϵ and at this order we have $\theta(+\infty) = \theta(-\infty)$ since the equations for the parameters of the soliton are the same as the one obtained in the adiabatic approximation (see the discussion at the end of Appendix B). Accordingly, E_{rad} in Eq.(56) being of order ϵ^2 should be neglected. Hence, at order ϵ nothing has occurred for the soliton's energy: this quantity is not modified by the collision with the obstacle and the radiated energy should be neglected. Thus, it seems that our first-order approach is unable to predict the amount of energy lost by the soliton during the collision with the obstacle.

However, as already remarked in the study of the scattering of bright solitons [42], one can circumvent this difficulty and extract some second-order information from our results. The procedure is the following: when pushing the computations at order ϵ^2 , the $\mathcal{O}(\epsilon^2)$ estimate of E_{rad} is still given by the second term on the RHS of (56) with $\delta\phi = \epsilon\phi_1$, which we know from our first-order approach. At second order, since E_{rad} is non zero, the soliton's energy has been modified by the collision and energy conservation now reads

$$\frac{4}{3} \cos^3[\theta(-\infty)] = E = \frac{4}{3} \cos^3[\theta(+\infty)] + E_{\text{rad}} . \quad (57)$$

Equation (57) allows us to determine the change in the soliton's parameter θ . Writing $\theta(-\infty) = \theta_0$ (with $\sin \theta_0 = V$) and $\theta(+\infty) = \theta_0 + \delta\theta$ one obtains

$$\delta\theta = \frac{E_{\text{rad}}}{4 \cos^2 \theta_0 \sin \theta_0} . \quad (58)$$

From Eq. (58) one can also determine the velocity at $t \rightarrow +\infty$ which is equal to $\sin[\theta(+\infty)] = V + \delta\theta \cos \theta_0$. Thus, we can determine how the collision has affected the soliton's shape and velocity by computing E_{rad} (replacing $\delta\phi$ by ϕ_1). This will be done in the remaining of this section.

On the basis of the analysis in terms of forward- and backward-emitted wave packet made in Section 4.3, one can separate E_{rad} into two parts, which we denote E_{rad}^- and E_{rad}^+ , the first one corresponding to energy radiated backwards and the second one to forward-radiated energy, with

$$E_{\text{rad}}^\alpha = \lim_{t \rightarrow +\infty} \frac{1}{2} \int_{\mathbb{R}} dx \left\{ |\delta\phi_x^\alpha|^2 + (\Phi^* \delta\phi^\alpha + \delta\phi^{\alpha*} \Phi)^2 \right\} . \quad (59)$$

A long computation which is summarized in Appendix C yields the result

$$E_{\text{rad}}^{\alpha} = 16 \pi \int_0^{+\infty} dq |D_q^{\alpha}(+\infty)|^2 (\varepsilon_q^{\alpha})^2 \left(\frac{q^2}{4} + 1 \right). \quad (60)$$

When $D_q^{\alpha}(+\infty)$ is given by Eq.(38), one obtains

$$E_{\text{rad}}^{\alpha} = \frac{\pi}{16 V^6} \int_0^{+\infty} dq \frac{q^2 (\varepsilon_q^{\alpha})^2 |\hat{U}(\varepsilon_q^{\alpha}/V)|^2}{\sinh^2 \left(\frac{\pi q \sqrt{1 + q^2/4}}{2 V \sqrt{1 - V^2}} \right)}. \quad (61)$$

The behavior at low and high velocity of E_{rad}^{α} defined in Eq.(61) is the following

$$E_{\text{rad}}^{\alpha} \sim \frac{\pi}{16 V} \int_0^{+\infty} \frac{q^4 |\hat{U}(q)|^2}{\sinh^2 \left(\frac{\pi q}{2} \right)} dq \quad \text{when } V \rightarrow 0, \quad (62)$$

and

$$E_{\text{rad}}^{-} \sim \frac{4}{15} (1 - V^2)^{5/2} |\hat{U}(0)|^2, \quad E_{\text{rad}}^{+} \sim \frac{2}{35} (1 - V^2)^{9/2} |\hat{U}(0)|^2, \quad \text{when } V \rightarrow 1. \quad (63)$$

One sees from Eq. (62) that our approach predicts an unphysical divergence of the radiated energy at low incident soliton velocity. On the contrary, numerical computations indicate that a soliton with very low velocity does not radiate [21, 22]. However, one must bear in mind that (61) is the result of a first-order expansion only valid in the limit $V^2 \gg U$ and is unable to tackle the regime of very low incident velocities. More interestingly, in the high-velocity regime – where the first-order perturbation theory is valid – we see from Eq. (63) that the leading-order estimate of the total amount of radiation (forward or backward emitted) vanishes.

In order to fix the ideas, we plot in Fig. 6 the value of E_{rad}^{α} as a function of the initial soliton velocity V . The obstacle is here taken to be a *delta* scatterer $U(z) = \lambda \delta(z)$. In this case $\hat{U}(q) = \lambda$.

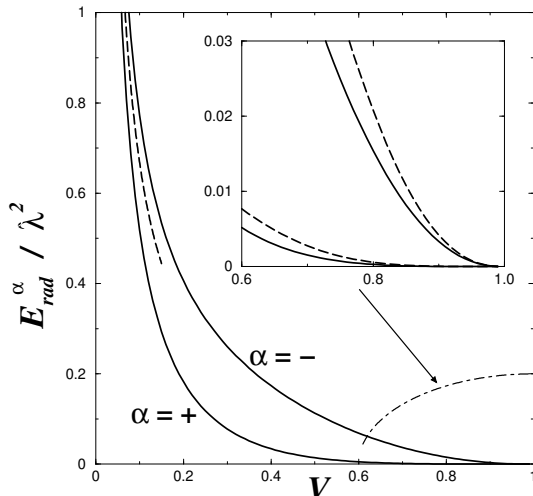


FIG 6. Energy E_{rad}^{α} radiated in the forward ($\alpha = +$) and backward ($\alpha = -$) directions by a soliton of initial velocity V incident on a δ scatterer. The solid lines represent the result (61) and the dashed line the approximation (62) which reads here $E_{\text{rad}}^{\alpha} \simeq \lambda^2/(15 V)$. The inset displays a blowup of the figure at high velocity. In the inset, the dashed curves are the asymptotic results (63).

Figure 6 shows that most of the energy is radiated backwards (this was already implicit in Fig. 5) and confirms that, at leading order in U/V^2 , a soliton does not radiate in the limit $V \rightarrow 1$. Besides, not only the absolute value of E_{rad} goes to zero, but also the relative amount of energy radiated E_{rad}/E vanishes [as $(1 - V^2)$]. Very similar results are obtained for an obstacle interacting with the beam through a finite-range potential (for instance, a Gaussian). This absence of radiation of a fast soliton can be explained intuitively as follows: whatever the sign of the potential describing the obstacle, the soliton loses energy under the form of radiated phonons. Accordingly it gets less dark [$\delta\theta > 0$ in Eq. (58)] and is accelerated. This increased velocity after a loss of energy is a typical feature of dark solitons which are sometimes referred to as effective particles having a negative kinetic mass which decreases with increasing energy [43]. However, our results show that, since the soliton velocity cannot exceed the speed of sound, a soliton whose velocity is close to this upper limit cannot be further accelerated and the radiative process is suppressed.

5 Conclusion

In this paper we have presented a study of the dynamics of a dark soliton experiencing a collision with a finite-size potential in a quasi-1D condensate. We determined the evolution of the soliton's parameters and also included radiative effects within secular perturbation theory.

A first output of the present work is what we called the “effective potential theory”: in many instances the soliton can be described as an effective classical particle of mass 2 (twice the mass of a bare particle) evolving in an effective potential U_{eff} [defined in Eq. (41)]. This approximation is rigorously valid in the case of a slow soliton incident on a weak potential, but its actual regime of validity appears to be quite broad.

The effective potential theory is an approximation where – as in all adiabatic approaches – radiative effects are neglected. Perturbation theory allows one to get a deeper insight into the collisional process and to determine the amount of radiated energy at leading order in U/V^2 . We show that the radiated waves form two counterpropagating phonon wave packets, and we predict that the radiative process is suppressed in the limit of a soliton moving with a velocity close to the velocity of sound. This result should be checked numerically; work in this direction is in progress.

Whereas adiabatic theory predicts that the soliton's shape and velocity are the same far before and far after the collision with the obstacle, it is an important feature of the perturbative approach of being able to determine finite asymptotic modifications of the soliton's parameters due to the collision. We computed [in Eq. (58)] the modification of the soliton's parameters at leading order in U/V^2 . The qualitative picture of the collisional process drawn from our approach is the following: the soliton radiates energy, gets less dark, and is accelerated. Since the velocity of a dark soliton cannot exceed the velocity of sound in the system, it is natural that this velocity appears as a threshold for emission of radiations. Roughly speaking, a soliton with a velocity close to the velocity of sound cannot radiate [as seen from Eqs. (63)] since its velocity cannot further increase.

Acknowledgments

It is a pleasure to thank E. Bogomolny, C. Schmit, G. Shlyapnikov, and C. Texier for fruitful discussions. We acknowledge support from CNRS and Ministère de la Recherche (Grant ACI

Appendix A

In this appendix we present the eigenvectors and eigenvalues of the Hamiltonian \mathcal{H} defined in Eq.(27). \mathcal{H} is not diagonalizable because, as we will see below, its null space and the one of \mathcal{H}^2 are not identical. If we denote by its “generalized null space” [37] the union of these two null spaces, one can easily verify that it is spanned by the four vectors $|\omega_o\rangle$, $|\omega_e\rangle$, $|\Omega_o\rangle$, and $|\Omega_e\rangle$ defined as

$$\begin{aligned} |\omega_o\rangle &= \begin{pmatrix} \Phi = \chi + i \sin \theta \\ -\Phi^* = -\chi + i \sin \theta \end{pmatrix}, \quad |\Omega_o\rangle = \begin{pmatrix} x \chi_x + \chi \\ x \chi_x + \chi \end{pmatrix}, \\ |\omega_e\rangle &= \begin{pmatrix} \Phi_x = \chi_x \\ \Phi_x = \chi_x \end{pmatrix}, \quad |\Omega_e\rangle = \begin{pmatrix} i \cos \theta \Phi_\theta = -\cos^2 \theta - i \sin \theta (x \chi_x + \chi) \\ i \cos \theta \Phi_\theta^* = \cos^2 \theta - i \sin \theta (x \chi_x + \chi) \end{pmatrix}, \end{aligned} \quad (\text{A1})$$

where the function $\chi(x, \theta)$ is defined in Eq.(14). The kets defined in Eq.(A1) verify $\mathcal{H}|\omega_o\rangle = \mathcal{H}|\omega_e\rangle = 0$ and $\mathcal{H}^2|\Omega_o\rangle = \mathcal{H}^2|\Omega_e\rangle = 0$, with $\mathcal{H}|\Omega_o\rangle = 2 \cos^2 \theta |\omega_o\rangle$ and $\mathcal{H}|\Omega_e\rangle = \cos^2 \theta |\omega_e\rangle$. One sees from Eq.(A1) that $|\omega_e\rangle$ and $|\Omega_e\rangle$ are, respectively, linked to variations of the center of the soliton and of the parameter θ (i.e., to the phase change across the soliton): this is the reason why the terms in θ_{t_1} and \bar{z}_{t_1} in Eq. (25) can be rewritten in Eq. (26) by means of $|\omega_e\rangle$ and $|\Omega_e\rangle$. One can similarly show that $|\omega_o\rangle$ is linked to modulations of the global phase of the soliton and that $|\Omega_o\rangle$ is linked to variations of the background density at infinity.

The remainder of the spectrum of \mathcal{H} is what we call the “phonon spectrum.” It has two branches which we denote “+” and “-.” The corresponding eigenvectors and eigenvalues are denoted $|\Xi_q^\pm\rangle$ and ε_q^\pm with

$$\mathcal{H} |\Xi_q^\pm\rangle = \varepsilon_q^\pm |\Xi_q^\pm\rangle. \quad (\text{A2})$$

The explicit expression of the eigenvalues is given in the main text [Eq. (32)]. It can be simply obtained by considering the form of Eq. (A2) when $x \rightarrow \pm\infty$. In this limit, Φ goes to a constant, and looking for the eigenvectors under the form of plane waves, $\exp\{i q x\} (U_q^\pm, V_q^\pm)^T$ (where U_q^\pm and V_q^\pm are constants), yields the result (32). This is the reason why we denote these excitations as phonons. A better denomination should be “Bogoliubov excitations” because, far from the soliton, their form and dispersion relation correspond indeed to the elementary excitations of a constant background moving with velocity $-V$.

The exact expression (valid for all $x \in \mathbb{R}$) of the eigenvectors is given by the squared Jost solutions of the inverse problem [23]. They read $|\Xi_q^\pm\rangle = (u_q^\pm(x), v_q^\pm(x))^T$ with

$$\begin{aligned} u_q^\pm(x) &= \exp\{i q x\} \left(\frac{q}{2} + \frac{\varepsilon_q^\pm}{q} + i \chi \right)^2, \\ v_q^\pm(x) &= \exp\{i q x\} \left(\frac{q}{2} - \frac{\varepsilon_q^\pm}{q} + i \chi \right)^2. \end{aligned} \quad (\text{A3})$$

The natural inner product of two kets is $\langle \cdot | \sigma_3 | \cdot \rangle$, where σ_3 is the third Pauli matrix. The eigenvectors have the following normalization:

$$\langle \Xi_p^\beta | \sigma_3 | \Xi_q^\alpha \rangle = \int_{\mathbb{R}} dx [u_p^{\beta*}(x)u_q^\alpha(x) - v_p^{\beta*}(x)v_q^\alpha(x)] = \mathcal{N}_q^\alpha \delta_{\alpha,\beta} \delta(p-q), \quad (\text{A4})$$

with

$$\mathcal{N}_q^\alpha = 16 \alpha \pi q \sqrt{\frac{q^2}{4} + 1} \left(\frac{\varepsilon_q^\alpha}{q} \right)^2. \quad (\text{A5})$$

In the main text we also use the following orthogonality relations:

$$\langle \omega_e | \sigma_3 | \omega_e \rangle = \langle \Omega_e | \sigma_3 | \Omega_e \rangle = \langle \omega_e | \sigma_3 | \Xi_q^\alpha \rangle = \langle \Omega_e | \sigma_3 | \Xi_q^\alpha \rangle = 0, \quad \langle \omega_e | \sigma_3 | \Omega_e \rangle = -4 \cos^3 \theta \quad (\text{A6})$$

and

$$\langle \omega_o | \sigma_3 | \omega_o \rangle = \langle \omega_o | \sigma_3 | \omega_e \rangle = \langle \omega_o | \sigma_3 | \Xi_q^\alpha \rangle = 0, \quad \langle \omega_o | \sigma_3 | \Omega_e \rangle = 2i \sin \theta \cos \theta. \quad (\text{A7})$$

Appendix B

In this appendix we briefly present the Lagrangian approach for dark soliton of Kivshar and Królikowski [14] and derive the Lagrange equations (B9) and (B10).

In absence of the perturbation $R[\phi]$, Eq. (11) can be derived from the following Lagrangian density:

$$\mathcal{L}[\phi, \phi^*] = \frac{i}{2} (\phi^* \phi_t - \phi \phi_t^*) \left(1 - \frac{1}{|\phi|^2}\right) - \frac{1}{2} |\phi_z|^2 - \frac{1}{2} (|\phi|^2 - 1)^2. \quad (\text{B1})$$

Accordingly, the energy and momentum are defined by

$$\begin{aligned} E &= \int_{-\infty}^{+\infty} dz \left[\phi_t \frac{\partial \mathcal{L}}{\partial \phi_t} + \phi_t^* \frac{\partial \mathcal{L}}{\partial \phi_t^*} - \mathcal{L} \right] = \frac{1}{2} \int_{-\infty}^{+\infty} dz [|\phi_z|^2 + (|\phi|^2 - 1)^2], \\ P &= \int_{-\infty}^{+\infty} dz \left[\phi_z \frac{\partial \mathcal{L}}{\partial \phi_t} + \phi_z^* \frac{\partial \mathcal{L}}{\partial \phi_t^*} \right] = \frac{i}{2} \int_{-\infty}^{+\infty} dz (\phi \phi_z^* - \phi^* \phi_z) \left(1 - \frac{1}{|\phi|^2}\right). \end{aligned} \quad (\text{B2})$$

The Lagrangian density (B1) is not *a priori* the most natural one leading to Eq. (11), but for the asymptotic boundary condition we are working with ($|\phi| \rightarrow 1$ when $z \rightarrow \pm\infty$), it yields a finite value of the energy and, besides, the energy and momentum are now, for a field of the form $\phi(x - Vt)$ (in particular, in the case of a soliton), related by the relation $\delta E = V \delta P$, indicating that the background contribution has been removed and allowing one to treat the soliton as a classical particle-like object [33, 44]. For completeness, we note that, for a soliton, ϕ is given by Eq.(13) and its energy and momentum defined in Eq.(B2) have the following expressions:

$$E = \frac{4}{3} \cos^3 \theta, \quad P = \pi - 2\theta - \sin(2\theta). \quad (\text{B3})$$

Following Kivshar and Królikowski [14], one can obtain adiabatic equations of motion for the soliton's parameters in the following way. Let us consider a variational approximation of the type of Eq. (16); the field of the soliton is parametrized with time dependent quantities $q_1(t), \dots, q_n(t)$ and has no other time dependence: $\phi_{\text{sol}}(z, t) = \phi(z, q_1(t), \dots, q_n(t))$. One first defines the Lagrangian for the q_i 's as being

$$L(q_1, \dot{q}_1, \dots, q_n, \dot{q}_n) = \int_{-\infty}^{+\infty} dz \mathcal{L}[\phi_{\text{sol}}, \phi_{\text{sol}}^*]. \quad (\text{B4})$$

Then the quantities $\partial_{q_i} L$ and $\partial_{\dot{q}_i} L$ are computed via

$$\partial_{q_i} L = \int_{-\infty}^{+\infty} dz (\partial_{q_i} \phi \partial_{\phi} \mathcal{L} + \partial_{q_i} \phi_z \partial_{\phi_z} \mathcal{L} + \partial_{q_i} \phi_t \partial_{\phi_t} \mathcal{L}) + \text{c.c.} \quad (\text{B5})$$

and

$$\partial_{\dot{q}_i} L = \int_{-\infty}^{+\infty} dz \partial_{\dot{q}_i} \phi_t \partial_{\phi_t} \mathcal{L} + \text{c.c.} \quad (\text{B6})$$

where c.c. stands for complex conjugate. Considering that ϕ is solution of Eq.(11) (including the perturbative term $R[\phi]$), simple manipulations allow one to obtain Lagrange-like equations for the q_i 's:

$$\begin{aligned} \partial_{q_i} L - \frac{d}{dt}(\partial_{\dot{q}_i} L) &= \int_{-\infty}^{+\infty} dz [\partial_{\phi} \mathcal{L} - \partial_z(\partial_{\phi_z} \mathcal{L}) - \partial_t(\partial_{\phi_t} \mathcal{L})] \partial_{q_i} \phi + \text{c.c.} \\ &= 2 \text{Re} \left\{ \int_{-\infty}^{+\infty} dz R^*[\phi_{\text{sol}}] \partial_{q_i} \phi_{\text{sol}} \right\}. \end{aligned} \quad (\text{B7})$$

In the particular case where $\phi_{\text{sol}}(z, t) = \Phi(z - \bar{z}(t), \theta(t))$ one obtains

$$L(\theta, \dot{\theta}, \bar{z}, \dot{\bar{z}}) = \dot{\bar{z}} [\pi - 2\theta - \sin(2\theta)] - \frac{4}{3} \cos^3 \theta, \quad (\text{B8})$$

and the equations of motion (B7) read explicitly

$$4 \dot{\theta} \cos^2 \theta = 2 \text{Re} \left\{ \int_{-\infty}^{+\infty} dz R^*[\phi_{\text{sol}}] \partial_{\bar{z}} \phi_{\text{sol}} \right\} \quad (\text{B9})$$

and

$$4 \cos^2 \theta (\sin \theta - \dot{\bar{z}}) = 2 \text{Re} \left\{ \int_{-\infty}^{+\infty} dz R^*[\phi_{\text{sol}}] \partial_{\theta} \phi_{\text{sol}} \right\}. \quad (\text{B10})$$

We note here a general feature, always valid in the framework of the adiabatic approximation: with equation (4) conserving energy, one can show that the soliton's energy defined in Eq.(B2) has the same value far before and far after the collision with the obstacle (the demonstration is essentially the same as the one given in Section 4.4 where, in addition, the consequences of soliton's radiation – neglected in the present adiabatic approximation – are taken into account). As a result, one obtains for the solutions of Eqs(B9) and (B10) that $\theta(+\infty) = \theta(-\infty)$, and $\dot{\bar{z}}(\pm\infty) = \sin \theta(\pm\infty) = V$. Hence the soliton's shape and velocity may change during the collision, but they eventually regain their initial values. This is intimately connected to the neglecting of radiative effects in the adiabatic approximation.

Appendix C

In this appendix we briefly indicate how to obtain expression (60) for the radiated energy starting from Eq.(59), where $\delta\phi$ is given by ϕ_1 -i.e., by (50). Instead of giving a detailed explanation on how to treat all the terms in the integrand of (59), for brevity we focus on one of the contributions to the expression (59) for E_{rad}^α :

$$\int_{-\infty}^{+\infty} dx |\Phi|^2 |\delta\phi^\alpha|^2 = \int_{-\infty}^{+\infty} dx \left(1 - \frac{\cos^2 \theta}{\cosh^2(x \cos \theta)} \right) |\phi_1^\alpha(x, t)|^2. \quad (\text{C1})$$

We recall that we are interested of the evaluation of this term at large times. Expressing ϕ_1 through Eq.(50), one can show that the term in \cosh^{-2} in the integrand on the RHS of Eq.(C1) can be dropped because it gives a contribution which decreases algebraically at $t \rightarrow +\infty$ (this can be checked by a stationary phase evaluation of the integrals over the momenta). It thus remains to evaluate

$$\int_{-\infty}^{+\infty} dx |\phi_1^\alpha|^2 = \int_{-\infty}^{+\infty} dq \int_{-\infty}^{+\infty} dp \int_{-\infty}^{+\infty} dx \{ C_q^\alpha C_p^{\alpha*} (u_q^\alpha u_p^{\alpha*} - v_q^{\alpha*} v_p^{\alpha}) + C_q^\alpha C_p^{\alpha*} v_q^\alpha v_p^{\alpha*} \}. \quad (\text{C2})$$

In Eq.(C2) we have added and subtracted the contribution $v_q^{\alpha*} v_p^{\alpha*}$ in order to make use of the normalization (A4). For the evaluation of the last part of the integrand on the RHS of Eq.(C2), the explicit expressions (A3) of $u_q^\alpha(x)$ and $v_q^\alpha(x)$ are to be used. In the course of this computation, an argument of stationary phase shows that only the x -independent terms with $p = q$ give a finite contribution at $t \rightarrow +\infty$. These terms will contribute as $2\pi\delta(p - q)$ after the integration over x . Altogether one obtains the expression

$$\int_{-\infty}^{+\infty} dx |\phi_1^\alpha|^2 \underset{t \rightarrow +\infty}{\simeq} \int_{-\infty}^{+\infty} dq |C_q^\alpha|^2 \left\{ \mathcal{N}_q^\alpha + 2\pi \left[\left(\frac{q}{2} - \frac{\varepsilon_q^\alpha}{q} \right)^2 + \cos^2 \theta \right]^2 \right\}. \quad (\text{C3})$$

Noting that \mathcal{N}_q^α defined in Eqs(A4) and (A5) is an odd function (and thus does not contribute to the integral since $|C_q^\alpha|^2$ is even) and explicitly computing the other contributions, one obtains

$$\int_{-\infty}^{+\infty} dx |\phi_1^\alpha(x, t)|^2 \underset{t \rightarrow +\infty}{\simeq} 8\pi \int_0^{+\infty} dq (q^2 + 2) \left(\frac{\varepsilon_q^\alpha}{q} \right)^2 |D_q^\alpha(+\infty)|^2. \quad (\text{C4})$$

The others contributions to Eq.(59) can be computed similarly. One obtains

$$\int_{-\infty}^{+\infty} dx |\partial_x \phi_1^\alpha|^2 \underset{t \rightarrow +\infty}{\simeq} 8\pi \int_0^{+\infty} dq q^2 (q^2 + 2) \left(\frac{\varepsilon_q^\alpha}{q} \right)^2 |D_q^\alpha(+\infty)|^2 \quad (\text{C5})$$

and

$$\int_{-\infty}^{+\infty} dx (\Phi^* \phi_1^\alpha)^2 \underset{t \rightarrow +\infty}{\simeq} -16\pi \int_0^{+\infty} dq \left(\frac{\varepsilon_q^\alpha}{q} \right)^2 |D_q^\alpha(+\infty)|^2. \quad (\text{C6})$$

Gathering all these contributions yields the final result (60).

References

- [1] W. Hänsel, P. Hommelhoff, T. W. Hänsch, and J. Reichel, *Nature (London)* **413**, 498 (2001); K. Bongs *et al.*, *Phys. Rev. A* **63**, 031602(R) (2001); H. Ott, J. Fortagh, G. Schlotterbeck, A. Grossmann, and C. Zimmermann, *Phys. Rev. Lett.* **87**, 230401 (2001); T. L. Gustavson *et al.*, *ibid* **88**, 020401 (2001); A. E. Leanhardt *et al.*, *ibid* **89**, 040401 (2002); J. Fortágh *et al.*, *Appl. Phys. Lett.* **81**, 1146 (2002); S. Schneider *et al.*, *Phys. Rev. A* **67**, 023612 (2003); Y. J. Lin, I. Teper, C. Chin, and V. Vuletić, *Phys. Rev. Lett.* **92**, 050404 (2004); T. Lahaye *et al.*, *ibid* **93**, 093003 (2004).
- [2] Y. Shin *et al.*, *Phys. Rev. Lett.* **92**, 050405 (2004).
- [3] M. Cristiani, O. Morsch, J. H. Müller, D. Ciampini, and E. Arimondo, *Phys. Rev. A* **65**, 063612 (2002); O. Morsch, J. H. Müller, M. Cristiani, D. Ciampini, and E. Arimondo, *Phys. Rev. Lett.* **87**, 140402 (2001).
- [4] B. P. Anderson and M. A. Kasevich, *Science* **282**, 1686 (1998); F. S. Cataliotti *et al.*, *ibid* **293**, 843 (2001).
- [5] C. Raman *et al.*, *Phys. Rev. Lett.* **83**, 2502 (1999); R. Onofrio *et al.*, *Phys. Rev. Lett.* **85**, 2228 (2000); S. Inouye *et al.*, *ibid* **87**, 080402 (2001).
- [6] L. Khaykovich *et al.*, *Science* **296**, 1290 (2002); K. E. Strecker, G. B. Partridge, A. G. Truscott, and R. G. Hulet, *Nature (London)* **417**, 150 (2002).
- [7] S. Burger *et al.*, *Phys. Rev. Lett.* **83**, 5198 (1999); J. Denschlag *et al.*, *Science* **287**, 97 (2000); Z. Dutton, M. Budde, C. Slowe, and L. V. Hau, *ibid* **293**, 663 (2001).
- [8] J. P. Keener and D. W. McLaughlin, *Phys. Rev. A* **16**, 777 (1977).
- [9] Y. S. Kivshar and B. A. Malomed, *Rev. Mod. Phys.* **61**, 763 (1989).
- [10] V. I. Karpman, *Phys. Scr.* **20**, 462 (1979).
- [11] D. J. Kaup and A. C. Newell, *Proc. R. Soc. London, Ser A* **361**, 413 (1978).
- [12] D. J. Kaup, *Phys. Rev. A* **42**, 5689 (1990); **44**, 4582 (1991).
- [13] Y. S. Kivshar and X. Yang, *Phys. Rev. E* **49**, 1657 (1994).
- [14] Y. S. Kivshar and W. Królikowski, *Opt. Commun.* **114**, 353 (1995).
- [15] V. V. Konotop, V. M. Pérez-García, Y.-F. Tang, and L. Vázquez, *Phys. Lett. A* **236**, 314 (1997).
- [16] T. Busch and J. R. Anglin, *Phys. Rev. Lett.* **84**, 2298 (1999).
- [17] D. J. Frantzeskakis, G. Theocharis, F. K. Diakonov, Peter Schmelcher, and Y. S. Kivshar, *Phys. Rev. A* **66**, 053608 (2002).

- [18] V. A. Brazhnyi and V. V. Konotop, Phys. Rev. A **68**, 043613 (2003).
- [19] V. V. Konotop and L. Pitaevskii, Phys. Rev. Lett. **93**, 240403 (2004).
- [20] S. Burtsev and R. Camassa, J. Opt. Soc. Am. B **14**, 1782 (1997).
- [21] N. G. Parker, N. P. Proukakis, M. Leadbeater, and C. S. Adams, J. Phys. B **36**, 2891 (2003).
- [22] N. G. Parker, N. P. Proukakis, and C. S. Adams, Chapter for the book "Progress in Soliton Research", Nova Publishing (New York) to appear.
- [23] X.-J. Chen, Z-D Chen, and N.-N. Huang, J. Phys. A **31**, 6929 (1998).
- [24] N.-N. Huang, S. Chi, and X.-J. Chen, J. Phys. A **32**, 3939 (1999).
- [25] V. V. Konotop and V. E. Vekslerchik, Phys. Rev. E **49**, 2397 (1994).
- [26] C. Menotti and S. Stringari, Phys. Rev. A **66**, 043610 (2002).
- [27] A. D. Jackson, G. M. Kavoulakis, and C. J. Pethick, Phys. Rev. A **58**, 2417 (1998).
- [28] M. Olshanii, Phys. Rev. Lett. **81**, 938 (1998).
- [29] P. Leboeuf and N. Pavloff, Phys. Rev. A **64**, 033602 (2001).
- [30] Nonstationary solutions do not fulfill Eq. (3) for the two following reasons: (i) at times when the perturbation of density reaches $x \rightarrow \pm\infty$, the density of nonstationary solutions will not exactly equal n_∞ far from the obstacle, and (ii) an additional phase difference (typically time dependent) will appear between $x \rightarrow -\infty$ and $x \rightarrow +\infty$ (such as the one which occurs in presence of a soliton).
- [31] D. S. Petrov, G. V. Shlyapnikov, and J. T. M. Walraven, Phys. Rev. Lett. **85**, 3745 (2000).
- [32] V. Hakim, Phys. Rev. E **55**, 2835 (1997).
- [33] Y. S. Kivshar and B. Luther-Davies, Phys. Rep. **298**, 81 (1998).
- [34] In dimensioned units, the velocity of sound in an unperturbed system of constant density n_∞ is $c = (2\hbar\omega_\perp a_{sc}n_\infty/m)^{1/2}$.
- [35] The fact that \bar{z} depends on the fast time t_0 may seem strange at first sight. This dependence is introduced in order to account for its behavior in absence of obstacle: $\bar{z} = V t$.
- [36] This is not the only possible way of writing the solution of Eq.(23). With the same degree of accuracy one can equivalently write $\bar{z} = \int^{t_0} \sin[\theta(\epsilon t'_0)] dt'_0 + \hat{z}(t_1)$, where \hat{z} is a (still unknown) function of t_1 .
- [37] M. I. Weinstein, SIAM J. Math. Anal. **16**, 472 (1985).
- [38] In dimensioned units this corresponds to a potential which varies slowly over a lengths scale of order of the healing length of the system.

- [39] A. E. Muryshev, H. B. van Linden van den Heuvell, and G. V. Shlyapnikov, Phys. Rev. A **60**, R2665 (1999).
- [40] Note that τ is very close to the actual time t and that, here, $t = 0$ corresponds to the time where the soliton's center would be at $z = 0$ in absence of the obstacle.
- [41] At these points the two saddles coalesce to $q_\alpha = 0$ and go to imaginary axis.
- [42] Y. S. Kivshar, A. M. Kosevich, and O. A. Chubykalo, Zh. Eksp. Teor. Fiz. **93**, 968 (1987) [Sov. Phys. JETP **66**, 545 (1987)].
- [43] P. O. Fedichev, A. E. Muryshev, and G. V. Shlyapnikov, Phys. Rev. A **60**, 3220 (1999).
- [44] I. V. Barashenkov and E. Yu. Panova, Physica D **69**, 114 (1993).